Numerical processing of palaeostress results

Tobore Orife, Richard J. Lisle*

Laboratory for Strain Analysis, Department of Earth Sciences, P.O. Box 914, Cardiff University, Cardiff CF10 3YE, UK

Abstract

Statistical evaluation of the results of palaeostress analysis is hindered by the fact that the common fault-slip methods provide incomplete information about the stress tensor. Our favoured approach to solving this problem involves assigning nominal values to the missing components of the tensor to subsequently create a *normalised* palaeostress tensor. The proposed normalised stress is deviatoric and has an octahedral shear stress of unity. The difference between two normalised tensors can then be expressed by a single parameter, the *palaeostress difference*, *D*. This procedure facilitates the comparison of different palaeostress results, such as those calculated from different sites or those obtained from different inversion methods applied to the same data. A numerical entity termed *the palaeostress tensor average* is proposed to summarise collections of normalised palaeostress tensor results. Following the description of the palaeostress tensor average, end-member relationships between stress tensors have been used to identify the likely range of values for a proposed measure of dispersion within a sample of palaeostress tensors. Observations from a Monte-Carlo experiment are used as the basis for determining significant values of the dispersion measure. The proposed numerical measures may provide another tool to aid the scientific assessment of the interpretations of current palaeostress inversion solutions.
© 2002 Elsevier Science Ltd. All rights reserved.

Keywords: Palaeostress; Stress inversion; Stress tensor; Statistics

1. Introduction

Although a wide range of techniques have been developed for reconstructing palaeostresses from microstructures (Dunne and Hancock, 1994), the methods based on faults and their associated slip indicators, the so-called fault-slip methods, are by far the most popular (see Angelier, 1994; Ramsay and Lisle, 2000, pp. 785–810 for an exhaustive review). Hundreds of applications of fault-slip methods are described in the literature; many of these include regional surveys based on numerous sites (e.g. Bergerat, 1987; Hardcastle, 1989; Simón, 1989; Gudmundsson et al., 1992; Ratschbacher et al., 1993; Bellier and Zoback, 1995; Peresson and Decker, 1997; Ghisetti, 2000). Such fault-slip methods treat faults as natural shear stress gauges, the observed direction of slip being used to indicate the direction of the resolved shear stress vector that acted on the plane of the fault.

The field data employed in fault-slip analysis of palaeostresses consist solely of the orientations of fault planes and associated slip directions and therefore do not include information on shear stress magnitudes. For this reason, the analysis of stresses by stress inversion of these data does not permit the complete stress tensor, consisting of six independent quantities, to be determined. Instead, the results are limited to a *reduced tensor* (Angelier, 1989, 1994) composed of three variables specifying the orientation of the principal stress axes and a fourth variable, often called the stress ratio, that expresses the ratio of the differences between pairs of principal stress magnitudes.

This incomplete nature of the palaeostress tensor presents problems when different tensors are to be compared, for example the tensors resulting when one fault-slip data set is being analysed by two different inversion methods. There exists presently no objective way of assessing the difference between two stress determinations from fault-slip data, though Michael (1978a,b, 1991) has addressed this issue in relation to earthquake focal mechanisms. Any assessment based solely on orientation differences of the principal axes is hampered by the fact that, depending on the shape of the stress ellipsoids involved, the axes may not have well defined directions. For instance, if the stress states being compared

* Corresponding author. Tel.: +44-1222-874830; fax: +44-1222-874326.

E-mail addresses: lisle@cardiff.ac.uk (R.J. Lisle), orife@cardiff.ac.uk (T. Orife).

are of axial compression type (σ_2 and σ_3 close in magnitude), the direction of the principal axis of greatest compression will be intrinsically more stable than the directions of the other two principal axes and should be given greater weight in the comparison. This suggests that a comparison of two tensors should not be based purely on their directional attributes but must instead be based upon all six components of the respective tensors. This preferred approach is prevented by the incomplete nature of the stress tensors.

The calculation of an average palaeostress state is similarly hindered by the fact that fault-slip analyses do not yield the complete stress tensor. To obtain a description of the average stress for a region, some workers have resorted to separately averaging the individual principal stress directions, even though the mean axes so calculated do not possess the orthogonality property for principal directions (Lisle, 1989). Others have calculated variants of the arithmetic average of the stress ratios for different sites or methods (e.g. Hardcastle, 1989; Bellier et al., 1997; Orife et al., 2002).

In this paper, we outline methods for the manipulation of palaeostress results that circumvent these problems. The methods involve constructing, for each stress result, a normalised stress tensor composed of the four components determined from the stress inversion of fault data and supplemented by nominal values for the other two unknowns. This philosophy of substituting nominal values into the stress tensor is shared by the method described by Spang (1972) whose data from twinning in calcite yield estimates of only three components of the stress tensor; three other components had to be assumed to derive his numerical dynamic analysis tensor. Tensor differences and tensor averages are calculated from these normalised stress tensors.

This contribution is made with the knowledge that confidence limits for the stress axes inverted are seldom presented in the reporting of palaeostress solutions. However, it is our opinion that the observation of a mutual overlap in the confidence limits for the stress axes (where this is available) could be a useful qualifier of the difference between two stress solutions.

2. Components of the stress tensor

The stress tensor, the full specification of the state of stress at a point, is made up of six independent components. An alternative way of describing the stress is with reference to the principal stresses. According to this scheme, three quantities are required to specify the principal stress values and three are needed to describe the orientation of the principal stress axes relative to some geographical reference frame. The second formulation is advantageous in terms of ease of visualisation of the stress state. However, for the stresses estimated by fault-slip methods, this scheme based

on principal stress magnitudes is impractical because these methods do not permit the individual values of the principal stresses to be determined. Instead, the methods yield an estimate of the stress ratio that is a function of all three principal stresses. Rather than principal stresses therefore, the following three parameters are a more natural choice for the description of the magnitude of the palaeostresses responsible for bringing about slip on faults:

1. *Mean stress* ($\bar{\sigma}$). This parameter specifies the average level of normal stress acting on all potential fault planes. It governs the frictional resistance on fault planes to slip and equals the mean of the principal stresses magnitudes:

$$\bar{\sigma} = \frac{\sigma_1 + \sigma_2 + \sigma_3}{3} \tag{1}$$

2. *Octahedral shear stress* (τ_{oct}). This is a measure of the importance of the deviatoric component of the stress tensor and hence of the levels of shear stress produced by the stress state. In contrast to the mean stress this quantity is responsible for driving the slip on fault planes. It is defined as the value of shear stress acting on the octahedral plane, the plane inclined at equal angles with respect to all three principal stress directions (Nádai, 1937):

$$\tau_{oct} = \sqrt{\frac{(\sigma_1 - \sigma_2)^2 + (\sigma_2 - \sigma_3)^2 + (\sigma_1 - \sigma_3)^2}{3}} \tag{2}$$

It is interesting to note that the description of τ_{oct} in Eq. (2) shows a remarkable resemblance to equations formulated for the standard deviation measure used in the statistical description of dispersion.

3. *The stress ratio*. The stress ratio, Φ, is the ratio of principal stress differences. It controls, for any given plane, the direction of shear stress and determines the geometry of the slip on fault planes (Wallace, 1951; Bott, 1959). It is defined (Bishop, 1966; Angelier, 1975) as:

$$\Phi = \frac{\sigma_2 - \sigma_3}{\sigma_1 - \sigma_3} \tag{3}$$

The stress ratio describes the symmetry of the distribution of the principal stress values. It serves to locate the intermediate principal stress value within the interval defined by the maximum and minimum stress values. Continuing the statistics analogy, the stress ratio therefore resembles the skewness measure commonly used to assess asymmetry.

These chosen parameters ($\bar{\sigma}$, τ_{oct} and Φ) therefore have a direct bearing on mechanical and geometrical aspects of fault-slip yet fulfil the same role of defining the state of stress as the principal stress values σ_1, σ_2 and σ_3. Relationships between these six variables are derived in Appendix A. Fault-slip analysis allows Φ to be estimated but provides no indication of the magnitudes of the mean
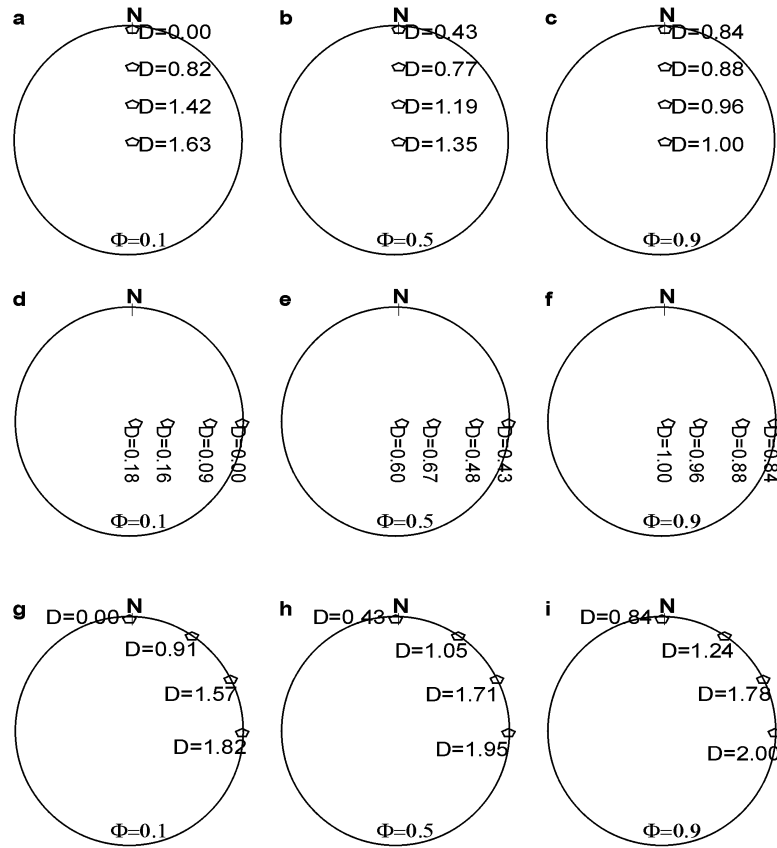
Fig. 1. Calibration of stress difference parameter, *D*. Stereograms showing systematic stress difference (*D*) variation between a 'fixed' stress tensor and a 'roaming' stress tensor. See text for further discussion. Fixed tensor is: $\sigma_1 = 000-00$; σ_2 is vertical; $\sigma_3 = 090-00$; $\Phi = 0.1$. Polygons on strereograms indicate stress axes orientation of σ_1 (or σ_3 as the case may be) and stress ratio values (*Φ*) for roaming tensors. All stereograms are lower hemisphere equal-area projections. Orientation details of roaming tensor are detailed below: (a)–(c): σ_2 is fixed to 090–00. σ_1 is varied from 000–00 to vertical through 000–30 and 000–60. (d)–(f): σ_1 is fixed to 000–00. σ_3 is varied from 090–00 to vertical through 090–30 and 090–60. (g)–(i): σ_2 is fixed to vertical. σ_1 is varied from 000–00 to 090–00 through 030–00 and 060–00.

stress or of the octahedral shear stresses. Therefore, in order to construct normalised stress tensors from fault-slip results we have to assign notional values to these missing quantities; we assume arbitrarily that $\bar{\sigma} = 0$ and $\tau_{oct} = 1$ stress unit.

The normalised tensor proposed here is identical to the 'unit deviator' defined by Ilyushin (1940) in connection with plastic deformation in metals. It is given by Nádai (1950, p. 107) in diagonalized form as:

$$\tau_{oct}^{-1} = \begin{bmatrix} \sigma_1 - \bar{\sigma} & 0 & 0 \\ 0 & \sigma_2 - \bar{\sigma} & 0 \\ 0 & 0 & \sigma_3 - \bar{\sigma} \end{bmatrix} \qquad (4)$$

Since the principal stresses are generally unknown in palaeostress analysis, this normalised palaeostress tensor is more usefully expressed in terms of *Φ*, i.e.:

$$k^{-1} \begin{bmatrix} 2 - \Phi & 0 & 0 \\ 0 & 2\Phi - 1 & 0 \\ 0 & 0 & -(\Phi + 1) \end{bmatrix} \qquad (5)$$

where $k = \sqrt{2\Phi^2 - 2\Phi + 2}$ (see Appendix A).

An alternative normalisation scheme by Etchecopar et al. (1981) produces reduced tensors from palaeostress results by assigning values of $\sigma_1 = 1$ and $\sigma_3 = 0$. This normalises the tensors in terms of differential stress though this advantage comes at the expense of a lack of uniformity of mean stress and octahedral shear stress. Angelier (1994) discusses other possible forms of the reduced stress tensor.

Details of the computer program that implement the numerical procedures proposed below are to be published separately as Lisle and Orife (2002). Copies of the program are available on request from the authors.

3. Difference between stress results

3.1. Theory

Stress superimposition, or calculating the result of combining two stress states each represented by a stress tensor, involves the arithmetic addition of corresponding components of the respective tensors to produce a new tensor representing the combined stress. From this basis, it is a logical step to define the difference between two stress
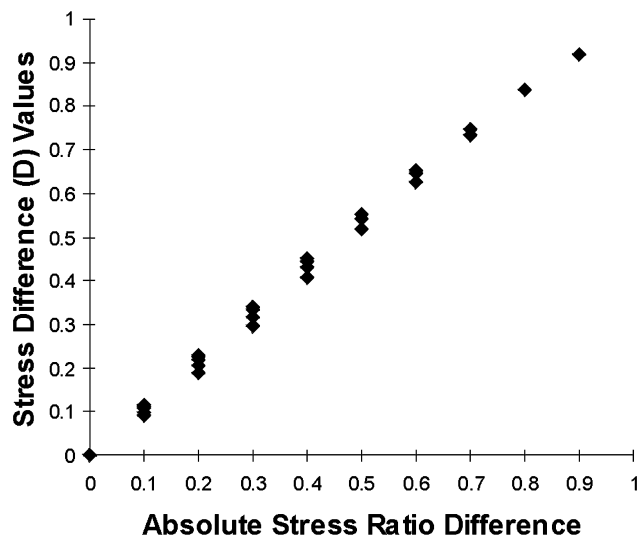
Fig. 2. Scatter-plot of stress ratio difference (absolute) against stress difference value (D) for pairs of co-axial stress tensors.

states as the result of subtraction of the two tensors. The difference between tensors $\boldsymbol{\sigma}_A$ and $\boldsymbol{\sigma}_B$ is therefore also a tensor $\boldsymbol{\sigma}_D$, called here the difference tensor:

$$\boldsymbol{\sigma}_D = \boldsymbol{\sigma}_A - \boldsymbol{\sigma}_B \qquad (6)$$

$\boldsymbol{\sigma}_D$ can itself be described by its principal directions, mean stress, octahedral shear stress, and stress ratio. When $\boldsymbol{\sigma}_A$ and $\boldsymbol{\sigma}_B$ are normalised tensors their difference tensor $\boldsymbol{\sigma}_D$ always has $\bar{\sigma}$ equal to zero. We propose the magnitude of the octahedral shear stress (τ_{oct}) of $\boldsymbol{\sigma}_D$ to be an appropriate measure of the magnitude of the difference between two palaeostress tensors. This scalar quantity is termed the *stress difference*, D.

It can be shown that D is zero where the two tensors are identical. D achieves a maximum value of 2.0 when $\boldsymbol{\sigma}_B = -\boldsymbol{\sigma}_A$. These tensors $-\boldsymbol{\sigma}_A$ and $\boldsymbol{\sigma}_A$ could be described as 'opposites' in the sense that their σ_1 and σ_3 axial directions are interchanged and their stress ratios are $1 - \Phi$ and Φ, respectively.

The tensor $-\boldsymbol{\sigma}_A$, in relation to $\boldsymbol{\sigma}_A$, has been previously termed the inverse tensor (Nemcok and Lisle, 1995) but in the language of matrices the term 'negative' palaeostress
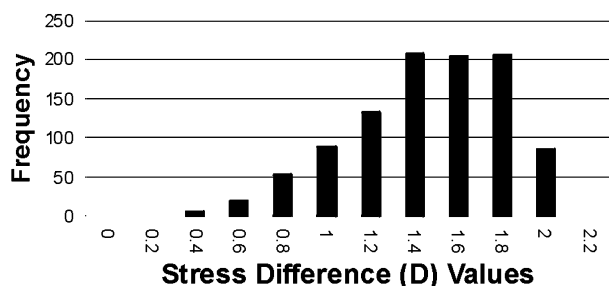

Fig. 3. Frequency histogram of stress difference (D) values for 1000 pairs of randomly selected stress tensors.

tensor is more appropriate (Ayres, 1974, p. 2). From inspection of Eq. (2), we can see that the order in which the tensors are subtracted from each other (in Eq. (6)) is unimportant.

3.2. Calibration of the proposed stress difference measure

To gain an appreciation of the significance of different D values, a calibration exercise was done. The calibration of the stress difference was based on an experiment that involved comparing a 'fixed' stress tensor with a 'roaming' stress tensor that is varied in a systematic way. The experiment was in essence set up to investigate the behaviour of the stress difference, D under restricted end-member conditions. For the sake of simplicity, the stress tensors are forced to share one common axis whilst the other two axes as well as the stress ratio of the roaming tensor were varied. Our observations from this exercise are summarised in Fig. 1.

The stereoplots of Fig. 1 indicate that as the roaming tensor is varied in a systematic way, the stress difference measure (D) also varies systematically. This measure can be calibrated by considering the following three cases:

1. Where the tensors are identical (i.e. the tensors are coaxial and possess identical stress ratios) a D value of zero is obtained (Fig. 1a, d and g);
2. Where the tensors are most different (i.e. where the tensors are opposites or 'negative' of each other) a D value of two results (Fig. 1i) and;
3. Where the sum of the stress ratios of both tensors equal unity and the σ_1 (or σ_3) axes are interchanged with the σ_2 axis for one of the tensors yielding a D value of one (Fig. 1c and f).

In addition, Fig. 2 indicates that where coaxial stress tensors are analysed, the absolute value of stress ratio difference is a first approximation to the tensor difference measure D.

From these tests, we conclude that the stress difference D is a systematic representation of the difference between any two palaeostress tensors.

3.3. How are D values distributed for randomly selected pairs of stress tensors?

We undertook an experiment that involved observing D values determined by analysis of the difference between random pairs of tensors. The experiment was aimed at devising qualitative terms to express the difference between palaeostress tensors and establishing the range of values of D to be expected from random palaeostress tensors. This was done in order to explore the usefulness of D as a test statistic of randomness of palaeostress results.

This Monte-Carlo experiment involved generating

Table 1
Terms proposed for a qualitative description of stress difference (*D*) between two stress tensors

Qualitative descriptor	Statistical definition of range for qualitative descriptor	Range of stress ratio (*D*) values
Very different	Very different > (mean + 1S.D.)	>1.71
Different	(mean − 1S.D.) < Different < (mean + 1S.D.)	1.01–1.71
Similar	(mean − 2S.D.) < Similar < (mean − 1S.D.)	0.66–1.01
Very similar	Very similar < (mean − 2S.D.)	<0.66

randomly 2000 sets of stress axes that are then assigned a stress ratio (*Φ*) value randomly (thereby constructing 1000 pairs of tensors). These pairs of tensors were then subjected to the stress difference analysis. Stress difference (*D*) values obtained from this exercise have been statistically analysed (Fig. 3). In these experiments, *D* ranges from 0.21 to 1.98 with mean of 1.36, and a standard deviation of 0.35.

The difference values presented in Fig. 3 have been subjected to simple tests that suggest that the *D* values could have been drawn from a parent distribution that is approximately normal. Using boundary values based on an idealised normal distribution, we propose the terms in Table 1 to qualify the difference measure *D*. The boundary values for defining these terms are based on multiples of the standard deviation that are on either side of the mean value.

We propose that the *D* values presented in Table 2 are used as critical values (i.e. test statistics) for making decisions regarding the significance of differences between pairs of tensors. The critical values given in Table 2 can be used to test the hypothesis that the two tensors concerned are completely unrelated, as two tensors selected at random from a population characterised by equal frequency of axial orientation and stress ratios. This kind of test is illustrated using the two tensors depicted in Fig. 4. A visual inspection of Fig. 4 gives the impression that the tensors will differ greatly. The calculated *D* value for this pair of tensors is 0.661: they are therefore classified as 'similar' (Table 1). This value is lower than the 5% critical value (Table 2) and this therefore leads us to reject the hypothesis that the two are unrelated. Therefore contrary to first impressions the two tensors do not differ greatly. In other situations, where the obtained *D* value is very large, i.e. the tensors are markedly dissimilar; we are led to reject the hypothesis of two unrelated tensors.

Table 2
Critical values of stress difference *D* determined from Monte-Carlo simulations. These values can be used to test the hypothesis of two random tensors. Values listed are extreme values of *D*; values outside this range would lead to rejection of this hypothesis. See text for further discussion

1%	5%	10%	90%	95%	99%
0.4798	0.6862	0.8791	1.7837	1.8390	1.9464

4. Average palaeostress tensor

4.1. Theory

The specification of palaeostress results in the form of normalised tensors also permits the averaging of palaeostress results. Analogous to the arithmetic mean of scalar measurements, the average of *n* tensors is found by summation of corresponding components followed by division by *n*. Oertel (1981) and Brandon (1995) have employed the concept of *tensor average* in relation to finite strain. In their case too, the tensors concerned are incomplete necessitating nominal values of missing components to be assigned (by assuming no volume change).

After averaging of the normalised stress tensors to construct the *average tensor* (denoted for brevity as **σ**$_M$), the eigenvectors and eigenvalues of **σ**$_M$ can then be evaluated to find the principal stress axes orientations and principal stress magnitudes, respectively, of **σ**$_M$. It is important to note that the stress ratio of **σ**$_M$ is not equivalent to the arithmetic mean of the stress ratios of the component stress tensors.

4.2. The significance of the octahedral shear stress of **σ**$_M$

For the sake of brevity in the following discussion, the tensors that are averaged to construct **σ**$_M$ are simply called
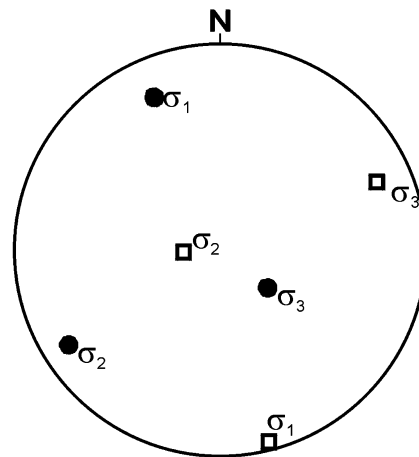

Fig. 4. Example of data used to calculate stress difference *D*. Two tensors are depicted in this stereogram. Lower hemisphere, equal area projection. Tensor 1 (filled circles): $\sigma_1 = 336$–18; $\sigma_3 = 128$–68; $\Phi = 0.08$. Tensor 2 (open squares): $\sigma_1 = 165$–02; $\sigma_3 = 065$–19; $\Phi = 0.12$.

Table 3
Table of proposed significant values of τ_{octM} determined from Monte-Carlo simulations. N = sample size, P = probability that τ_{octM} for a randomly generated sample of stress tensors is less than proposed significant value. See text for further discussion

P	$N = 2$	$N = 4$	$N = 6$	$N = 8$	$N = 10$	$N = 20$	$N = 50$	$N = 100$	$N = 1000$	$N = 10{,}000$
0.99	0.97492	0.77860	0.66712	0.57982	0.52842	0.40218	0.24172	0.17676	0.07024	0.02211
0.95	0.93083	0.71000	0.59313	0.50712	0.45464	0.33473	0.20547	0.15443	0.06176	0.01783
0.90	0.90253	0.67378	0.56207	0.47909	0.42479	0.30848	0.19223	0.14037	0.05586	0.01638

constituent tensors and the octahedral shear stress of $\boldsymbol{\sigma}_{\mathrm{M}}$ will be denoted by τ_{octM}.

Where two tensors are identical, $\boldsymbol{\sigma}_{\mathrm{M}}$ will be identical to the constituent stress tensors. It follows then that τ_{octM} will be exactly equal to the octahedral shear stress of the constituent tensors (i.e. τ_{octM} will be unity as specified in the normalisation).

Where two tensors that form opposites (i.e. a pair of tensors consisting of a tensor and its negative) are summed and averaged, the resulting tensor $\boldsymbol{\sigma}_{\mathrm{M}}$ is the null tensor. It is similarly trivial to show that the octahedral shear stress of the null tensor (i.e. τ_{octM}) is zero. We can conclude that values of τ_{octM} lie in the range zero to unity. The above conclusion suggests that

the value of τ_{octM} is a potential indicator of dispersion of the constituent tensors that make up $\boldsymbol{\sigma}_{\mathrm{M}}$; high dispersion (i.e. the constituent tensors are variable in character) is indicated by low values of τ_{octM}.

A Monte-Carlo experiment to elaborate these concepts was undertaken that involved recording values of τ_{octM} obtained from sample datasets consisting of N randomly generated constituent stress tensors. For each sample size ($N = 2, 4, 6, 8, 10, 20, 50, 100, 1000, 10{,}000$) a thousand datasets were generated. The experiment was also aimed at determining what range of values of τ_{octM} could be expected for randomly generated samples of constituent tensors. From these results, summarised in Table 3, we observe that the value of τ_{octM} decreases as the sample size of the
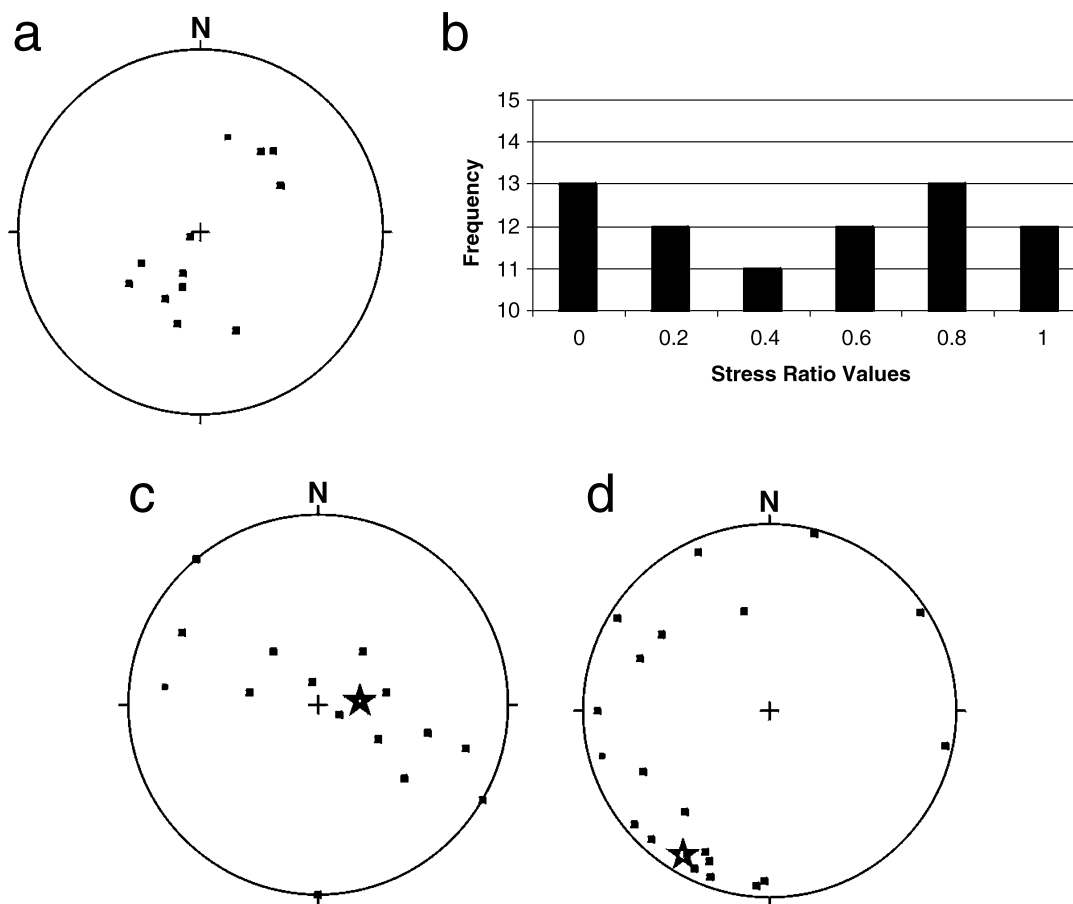

Fig. 5. Results of stress analysis based on slip-sense inversion. All stereograms are lower hemisphere, equal area projections. Polygons/stars in Fig.4c and d indicate orientation of σ_1 and σ_3 principal stress axes, respectively, for determined $\boldsymbol{\sigma}_{\mathrm{M}}$. See text for further discussion. Poles of faults for data published by Orife et al. (2002). All faults are normal ($N = 12$). Frequency histogram of stress ratio (Φ) values for compatible stress tensor solutions. Orientations of σ_1 stress axes for compatible solutions ($N = 73$). Orientations of σ_3 stress axes for compatible solutions ($N = 73$).

Table 4

Comparison of stress difference values for three different inversion algorithms used to analyse fault slip data presented in Fig. 3. $\boldsymbol{\sigma}_M$ is the average stress tensor determined for compatible solutions presented in Fig. 3. Bellier et al. (1989) is the inversion result obtained from original data. Row marked 'Program INVERS' is inversion result for original data from algorithm based on Sperner et al. (1993) (see text for discussion). Stress differences (D) between results of inversion algorithms and $\boldsymbol{\sigma}_M$ are presented under column marked D

Stress analysis	σ_1	σ_2	σ_3	Φ	D
$\boldsymbol{\sigma}_M$	085–72	304–14	211–11	0.34	–
Bellier et al. (1989)	098–64	287–26	195–04	0.46	0.331433
Program INVERS	097–71	277–19	007–00	0.429	0.364574

randomly generated datasets increases. This can be explained by the fact that a large sample of random tensors will produce an average tensor that approaches an isotropic tensor.

We propose that τ_{octM} values presented in Table 3 are used as critical values to make decisions regarding the significance of the τ_{octM} values obtained from natural samples. These values may help indicate preferred orientations and patterns during the analysis of palaeostress results.

5. Example application of proposed numerical measures

Applications of the numerical procedures proposed can be illustrated in the context of an analysis of the results of a stress inversion algorithm first proposed by Lisle et al. (2001) and later developed by Orife et al. (2002). The stress inversion criterion that these authors propose is based on the use of fault slip-sense to determine a range of compatible tensor solutions. Their method of stress inversion often yields large numbers of such compatible solutions. Their preferred method of presenting the inversion results were stereoplots showing the modal solutions of σ_1 and σ_3 stress axes, respectively, and a frequency histogram of the stress ratio values for compatible stress tensors. This form of presentation makes it difficult to compare the results of their method with those derived from other methods that yield single tensor solutions. To facilitate such comparisons we advocate that the potentially large numbers of solutions compatible with slip-sense data are summarised using the tensor average tool to aid the numerical manipulation and presentation of the results. Differences between the resulting average stress tensor derived from the slip-sense analysis and the results from other stress inversion methods can then be analysed using the difference tool.

We present here the numerical measures (D, $\boldsymbol{\sigma}_M$ and τ_{octM}) with the qualitative descriptions of D (Table 1) as an alternative to the preferred methods of Orife et al. (2002) for displaying the stress tensor results from a slip-sense inversion. The fault slip sense data (Fig. 5a) have been

presented by Orife et al. (2002) for a stress analysis based on the slip-sense inversion technique. The original data were presented by Bellier et al. (1989, fig. 11, site 10.3). We have re-analysed the published fault slip data of Orife et al. (2002, their table 2) using different input search parameters to those which they reported. Plots of compatible σ_1 and σ_3 orientations for the re-analysed data were obtained using the slip-sense inversion technique (Fig. 5c and d). A histogram of stress ratio values for the compatible solutions is also presented in Fig. 5b. We present in Fig. 5c and d and Table 4, the orientations of $\boldsymbol{\sigma}_M$ determined from the 73 compatible solutions for the data. A value of 0.639 for τ_{octM} was also determined for these compatible solutions. This value of τ_{octM} was compared with the appropriate values for datasets of comparable sample sizes presented in Table 3 (where N is between 50 and 100). The comparison suggests that the τ_{octM} value for the data is not typical of that expected from a random selection of stress tensors.

To illustrate the application of the stress difference D, we undertook a comparison between the average stress tensor for the data determined in the above analysis and the stress tensors that resulted from two other stress inversion attempts. One of the stress tensors was determined by Bellier et al. (1989, table 3) for the original data. The other stress tensor was also determined for the original data but using a stress inversion algorithm (INVERS) developed by Sperner et al. (1993). Although the results of the three methods intuitively appear to be rather similar (Table 4), we are now able to present appropriate numerical data to support the conclusion that the differences between the various inversion methods are relatively small. In the terminology proposed above for the qualitative description of stress difference, we describe the tensors as 'very similar' (Table 1). This example also illustrates the difference between the arithmetic mean of the stress ratio values (in this example 0.499) and the stress ratio of $\boldsymbol{\sigma}_M$ (i.e. 0.34; see Table 4).

6. Discussion

We do not believe that the examples presented above are an exhaustive list of the potential applications of the proposed numerical procedures. Other potential benefits of robust numerical comparisons (or summaries as the case may be) of palaeostress results include:

1. The identification of stress perturbations in a region under investigation. Practically, this could be achieved by inspecting the differences between an average stress tensor determined for the regional survey and the tensors determined for individual sites, and
2. Currently, there is a debate that surrounds the issue of validity (or otherwise) of palaeostress analysis (e.g. Marrett and Allmendinger, 1990; Twiss et al., 1991; Cladouhos and Allmendinger, 1993; Dupin et al., 1993; Pollard et al.,

1993; Twiss and Unruh, 1998; Fletcher and Pollard, 1999; Marrett and Peacock, 1999; Nieto-Samaniego, 1999; Tikoff and Wojtal, 1999; Gapais et al., 2000; Peacock and Marrett, 2000; Pollard, 2000; Roberts and Ganas, 2000). The consistency of palaeostress results may (or may not) provide arguments for determining the validity of palaeostress inversion techniques. The numerical procedures that we propose will assist in the development of objective tests for validity of interpretations of stress inversion solutions.

We urge caution in the interpretation of the average stress tensor. It remains to be seen how the average stress tensor relates to the bulk stresses that are applied to a volume of deforming rock (see Oertel (1981) for equivalent discussion of strain).

At this time, we are also uncertain about the value of determining the principal stress axes of the difference tensor.

7. Conclusions

We have attempted to overcome the problems associated with numerically processing and the comparison of palaeostress results, by proposing procedures that express numerically the difference between two palaeostress results to produce a quantity termed the *stress difference*. We also propose procedures to quantitatively summarise collections of palaeostress results in the form of an *average stress tensor*.

As by-products of these proposed numerical procedures, we further present qualitative descriptions of the stress difference values, and we describe a statistical measure to quantify the dispersion of the palaeostress results used in determining the average stress tensor.

It is our intention that the power of the proposed numerical measures will further enhance efforts to exploit the results of existing palaeostress surveys. Our hope is that this contribution will encourage further consensus amongst structural geologists regarding how such surveys may be improved in the future.

Acknowledgements

Appendix A. Principal stress values of the normalised palaeostress tensor

The normalised stress tensor is defined as having a mean stress equal to zero and an octahedral shear stress equal to unity.

Substituting $\bar{\sigma} = 0$ into Eq. (1) gives:

$$\sigma_3 = -(\sigma_1 + \sigma_2) \tag{A1}$$

Combining this with Eq. (3) gives:

$$\sigma_1 = \sigma_2 \left(\frac{2 - \Phi}{2\Phi - 1} \right) \tag{A2}$$

$$\sigma_1 - \sigma_2 = 3\sigma_2 \left(\frac{1 - \Phi}{2\Phi - 1} \right),$$

$$\sigma_2 - \sigma_3 = 3\sigma_2 \left(\frac{\Phi}{2\Phi - 1} \right),$$

$$\sigma_1 - \sigma_3 = 3\sigma_2 \left(\frac{1}{2\Phi - 1} \right).$$

Substituting into Eq. (2) and setting $\tau_{\text{oct}} = 1$ gives:

$$\sigma_2 = \frac{2\Phi - 1}{\sqrt{2\Phi^2 - 2\Phi + 2}} \tag{A3}$$

From Eq. (A2):

$$\sigma_1 = \frac{2 - \Phi}{\sqrt{2\Phi^2 - 2\Phi + 2}} \tag{A4}$$

and from Eq. (A1):

$$\sigma_3 = -\frac{\Phi + 1}{\sqrt{2\Phi^2 - 2\Phi + 2}} \tag{A5}$$

Though Φ is the most popular, the stress ratios below are used by different authors. These other stress ratios can be converted to Φ using:

R (Carey and Mercier 1987) $= (\sigma_2' - \sigma_1') / (\sigma_3' - \sigma_1') = (\sigma_1 - \sigma_2)/(\sigma_1 - \sigma_3)$
i.e. deviatoric stresses $\Phi = 1 - R_C$
R (Lisle, 1980) $= (\sigma_2 - \sigma_3)/(\sigma_1 - \sigma_2)$, $\Phi = R_L/(1 + R_L)$
μ (Nádai, 1950, p. 106) $= (2\sigma_2 - \sigma_1 - \sigma_3)/(\sigma_1 - \sigma_3)$, $\Phi = (\mu + 1)/2$

References

Angelier, J., 1975. Sur l'analyse de mesures recueillies sans des sites faillés: l'utilité d'une confrontation entre les méthodes dynamiques et cinématiques. Comptes Rendus de l'Académe des Sciences, Paris D281, 1805–1808.

Angelier, J., 1989. From orientation to magnitudes in paleostress

determination using fault slip data. Journal of Structural Geology 11 (2), 37–50.

Angelier, J., 1994. Fault slip analysis and palaeostress reconstruction. In: Hancock, P.L., (Ed.), Continental Deformation, Pergamon, pp. 53–100.

Ayres, F., 1974. Schaum's Theory and Problems of Matrices, McGraw-Hill, New York.

Bellier, O., Zoback, M.L., 1995. Recent state of stress change in the Walker–Lane Zone, Western Basin and Range Province, United States. Tectonics 14, 564–593.

Bellier, O., Sebrier, M., Fourtanier, E., Gasse, F., Robles, I., 1989. Late Cenozoic evolution of the E–W striking Cajamarca deflection in the Namora Basin (Andes of Northern Peru). Annales Tectonicæ 3 (2), 77–98.

Bellier, O., Över, S., Poisson, A., Andrieux, J., 1997. Recent temporal change in the stress state and modern stress field along the North Anatolian Fault Zone (Turkey). Geophysical Journal International 131, 61–86.

Bergerat, F., 1987. Stress fields in the European platform at the time of Africa–Eurasia collision. Tectonics 6, 99–132.

Bishop, A.W., 1966. The strength of soils as engineering materials. Géotechnique 16, 91–128.

Bott, M.H.P., 1959. The mechanics of oblique slip faulting. Geological Magazine 96, 109–117.

Brandon, M.T., 1995. Analysis of geologic strain in strain-magnitude space. Journal of Structural Geology 17, 1375–1385.

Carey, E., Mercier, J.L., 1987. A numerical method of determining the state of stress using focal mechanisms of earthquake populations: applications to Tibetan teleseisms and microseismicity of S Peru. Earth and Planetary Science Letters 82, 165–179.

Cladouhos, T.T., Allmendinger, R.W., 1993. Finite strain and rotation from fault-slip data. Journal of Structural Geology 15, 771–784.

Dunne, W.M., Hancock, P.L., 1994. Palaeostress analysis of small-scale brittle structures. In: Hancock, P.L., (Ed.), Continental Deformation, Pergamon, Oxford, pp. 101–120.

Dupin, J.M., Sassi, W., Angelier, J., 1993. Homogenous stress hypothesis and actual fault slip: a distinct element analysis. Journal of Structural Geology 15, 1033–1045.

Etchecopar, A., Vasseur, G., Daignieres, M., 1981. An inverse problem in microtectonics for the determination of stress tensors from fault striation analysis. Journal of Structural Geology 3, 51–65.

Fletcher, R.C., Pollard, D.D., 1999. Can we understand structural and tectonic processes and their products without appeal to a complete mechanics? Journal of Structural Geology 21, 1071–1088.

Gapais, D., Cobbold, P.R., Bourgeois, O., Rouby, D., de Urreiztieta, M., 2000. Tectonic significance of fault-slip data. Journal of Structural Geology 22, 881–888.

Ghisetti, F., 2000. Slip partitioning and deformation cycles close to major faults in southern California: evidence from small-scale faults. Tectonics 19 (1), 25–43.

Gudmundsson, A., Bergerat, F., Angelier, J., Villemin, T., 1992. Extensional tectonics of southwest Iceland. Bulletin de la Société Géologique de France 6 (11), 1555–1573.

Hardcastle, K., 1989. Possible palaeostress tensor configurations derived from fault-slip data in Eastern Vermont and Western New Hampshire. Tectonics 8 (2), 265–284.

Ilyushin, A.A., 1940. Deformation of plastico-viscous materials. Scientific Notes of the State University of Moscow, Russia. Issue 39.

Lisle, R.J., 1980. The representation and calculation of the deviatoric component of the geological stress tensor. Journal of Structural Geology 1, 317–321.

Lisle, R.J., 1989. The statistical analysis of orthogonal orientation data. Journal of Geology 97, 360–364.

Lisle, R.J., Orife, T., 2002. A QuickBasic program for numerical evaluation of palaeostress results. Computers and Geosciences in press.

Lisle, R.J., Orife, T., Arlegui, L., 2001. A stress inversion method requiring only fault slip sense. Journal of Geophysical Research 106 (B2), 2281–2289.

Marrett, R., Allmendinger, R.W., 1990. Kinematic analysis of fault-slip data. Journal of Structural Geology 12, 973–986.

Marrett, R., Peacock, D.C.P., 1999. Strain and stress. Journal of Structural Geology 21, 1057–1063.

Michael, A.J., 1987a. Use of focal mechanisms to determine stress: a control study. Journal of Geophysical Research 92 (B1), 357–368.

Michael, A.J., 1987b. Stress rotation during the Coalinga aftershock sequence. Journal of Geophysical Research 92 (B8), 7963–7979.

Michael, A.J., 1991. Spatial variations in stress within the 1987 Whittier Narrows, California, aftershock sequence: new techniques and results. Journal of Geophysical Research 96 (B4), 6303–6319.

Nádai, A., 1937. Plastic behaviour of metals in the strain-hardening range. Journal of Applied Physics 7, 205–213.

Nádai, A., 1950. Theory of Flow and Fracture of Solids, Vol. 1, McGraw-Hill, New York.

Nemcok, M., Lisle, R.J., 1995. A stress inversion procedure for polyphase fault/slip data sets. Journal of Structural Geology 17, 1445–1453.

Nieto-Samaniego, A.F., 1999. Stress, strain and fault patterns. Journal of Structural Geology 21, 1065–1070.

Oertel, G., 1981. Strain estimation from scattered observations in an inhomogeneously deformed domain of rocks. Tectonophysics 77, 133–150.

Orife, T., Arlegui, L., Lisle, R.J., 2002. DIPSLIP: a QuickBASIC stress inversion program for analyzing sets of faults without slip lineations. Computers and Geosciences 28, 775–781.

Peacock, D.C.P., Marrett, R., 2000. Strain and stress: reply. Journal of Structural Geology 22, 1369–1378.

Peresson, H., Decker, K., 1997. Far-field effects of Late Miocene subduction in the Eastern Carparthians: E–W compression and inversion of structures in the Alpine–Carpathian–Pannonian region. Tectonics 16, 38–56.

Pollard, D.D., 2000. Strain and stress: discussion. Journal of Structural Geology 22, 1359–1367.

Pollard, D.D., Saltzer, S.D., Rubin, A.M., 1993. Stress inversion methods; are they based on faulty assumptions? Journal of Structural Geology 15, 1045–1054.

Ramsay, J.G., Lisle, R.J., 2000. The Techniques of Modern Structural Geology. Volume 3: Applications of Continuum Mechanics in Structural Geology, Academic Press, London.

Ratschbacher, L., Linzer, H.G., Moser, F., Strusievicz, R.O., Bedelean, H., Har, N., Mogos, P.A., 1993. Cretaceous to Miocene thrusting and wrenching along the Central Carpathians due to a corner effect during collision and orocline formation. Tectonics 12 (4), 855–858.

Roberts, G.P., Ganas, A., 2000. Fault-slip direction in central and southern Greece measured from striated and corrugated fault planes: comparison with focal mechanism and geodetic data. Journal of Geophysical Research 105 (B10), 23443–23462.

Simón, J.L., 1989. Late Cenozoic stress field and fracturing in the Iberian Chain and Ebro Basin (Spain). Journal of Structural Geology 11, 285–294.

Spang, J.H., 1972. Numerical method for dynamic analysis of calcite twin lamallae. Geological Society of America Bulletin 83, 467–472.

Sperner, B., Ratschbacher, L., Ott, R., 1993. Fault striae analysis: a Turbo Pascal program package for graphical presentation and reduced stress tensor calculation. Computers and Geosciences 19, 1362–1388.

Tikoff, B., Wojtal, S.F., 1999. Displacement control of geologic structures. Journal of Structural Geology 21, 959–967.

Twiss, R.J., Unruh, J.R., 1998. Analysis of fault slip inversions; do they constrain stress or strain rate? Journal of Geophysical Research 103 (B6), 12205–12222.

Twiss, R.J., Protzman, G.M., Hurst, S.D., 1991. Theory of slickenline patterns based on the velocity gradient tensor and microrotation. Tectonophysics 186, 215–239.

Wallace, R.E., 1951. Geometry of shearing stress and relation to faulting. Journal of Geology 59, 118–130.